

<https://doi.org/10.29013/ELBLS-22-2-40-53>

Mingjia Fan,
Newton South High School,
140 Brandeis Road, Newton Centre, MA, USA, 02459
Moustafa Gabr,
Stanford University,
450 Serra Hall, Stanford, CA, USA, 94305

REPURPOSING OF KNOWN DRUGS AS POTENTIAL THERAPEUTICS FOR CANCER IMMUNOTHERAPY FOR PATIENTS WITH SOLID TUMORS

Abstract. For several decades treatment of advanced cancer has been challenged by lack of reliable therapeutic options. Patients with metastatic tumors that were not surgically resectable had to depend on chemotherapy, which is commonly associated with severe adverse events as well as high rates of relapse. As the understanding of immune system and immune surveillance grew, the idea of utilizing immune cells to eliminate cancer gained significance and various strategies to activate immune response were developed.

Tumor cells form immune escape and subsequently obtain unlimited proliferation ability due to the abnormal immune surveillance mediated by immune checkpoints. Negative immune checkpoints, such as programmed cell death protein 1 (PD-1), are regulators of human immune system that downregulate T-cell activation and hinder the ability of the immune system to attack cancer cells. FDA-approved monoclonal antibodies (mAbs) against negative immune checkpoints have revealed remarkable clinical success in different malignancies. However, there are currently no small molecules clinically approved based on targeting immune checkpoints. The aim of this project is to identify FDA-approved drugs that can be potentially used to target immune checkpoints and inhibit their function. The approach will be based on a computational study by investigating the ability of a library of known drugs to interact with the crystal structure of PD-1. This work would potentially enable the development of small molecules for early cancer diagnosis and personalized cancer immunotherapy.

Keywords: Immune Checkpoints, PD-1/PD-L1, Target, Small Molecule Inhibitors, Cancer Immunotherapy.

1. Introduction

Immune checkpoint molecules work as protective factors for the body's immune system [1]. However, when immune checkpoint molecules are overexpressed or overactivated, immune function is inhibited. The PD-1/PD-L1 signaling pathway was discovered relatively early. In the tumor microenvironment, activated T cells express high levels of PD-1

[2]. Upregulated PD-L1 prevents excessive activation of T cells, maintains the immune system's tolerance to self-antigens, and reduces the immune response against the surrounding normal tissue after combining with PD-1 on T cells via protein-protein interactions. Therefore, blocking the interaction of PD-1 and PD-L1 can reverse immunosuppressive conditions and improve the killing of tumor cells by the body's

immune cells. In recent years, anti-PD-L1 monoclonal antibodies have shown positive responses in clinical trials for a variety of malignancies, including melanoma, metastatic non-small-cell lung cancer, bladder cancer, and skin Merkel cell carcinoma [3; 4].

However, antibody drugs are associated with several disadvantages, such as immunogenicity issues and the poor permeability of tumor tissues, which lead to the overall low response rate of PD-1/PD-L1 antibody drugs [5]. Tumor cells continually activate the PD-1/PD-L1 signaling pathway by overexpressing PD-L1 to trigger multiple immune suppression mechanisms. From this perspective, this binding can also be interrupted by inhibiting the expression of PD-L1 or promoting its degradation. Increasing research is devoted to intervening in the PD-1/PD-L1 signaling pathway by applying small molecule compounds such as peptides and peptidomimetics to address this problem. Currently, these small molecular compounds are in the preclinical research stage. However, in some cases, malignant cells prohibit immune responses against tumors by upregulating immunosuppressive molecules or downregulating immune-activated molecules, thereby achieving immune escape and immortalization [6; 7]. PD-1/PD-L1 has been the most studied negative regulatory immune checkpoint-related axis in recent years and plays a prominent role in tumor immune escape [8; 9].

The purpose of my research paper is to focus on identifying FDA-approved drugs that can be potentially used to target immune checkpoints and inhibit their function. It would serve as starting points to designing more efficient inhibitors. The approach will be based on a computational study by investigating the ability of a library of known drugs to interact with the crystal structure of PD-1. This work would potentially enable the development of small molecules for early cancer diagnosis and personalized cancer immunotherapy.

2. Literature Review

For several decades treatment of advanced cancer has been challenged by lack of reliable therapeutic options. Patients with metastatic tumors that were

not surgically resectable had to depend on chemotherapy, which is commonly associated with severe adverse events as well as high rates of relapse. As the understanding of immune system and immune surveillance grew, the idea of utilizing immune cells to eliminate cancer gained significance and various strategies to activate immune response were developed [10; 11; 12]. However, the first generation of immunotherapies were limited by low response rates and high incidence of serious adverse events [13]. The search for dependable targets for the modulation of immune responses led to the discovery of checkpoints of T-cell activation and development of monoclonal antibodies targeting the checkpoints [14–20]. The impact of CTLA-4 and PD-1 blockers on cancer research and their success in cancer treatment is acknowledged by researchers as well as clinicians worldwide and rightfully the Nobel Prize in Physiology or Medicine for 2018 was awarded to Professor James Allison, MD Anderson Cancer Center, USA and Professor Tasuku Honjo, Kyoto University, Japan for their research on CTLA-4 and PD-1 respectively [21; 22].

For T cells, several regulatory mechanisms are induced during initial antigen-mediated activation, which involves peptide–MHC engagement of the T cell receptor (TCR) and positive costimulatory signals such as interactions between CD28 on T cells and CD80 and/or CD86 on antigen-presenting cells (APCs). Early during the activation process, negative regulators are induced to counteract the activation programme. Cytotoxic T lymphocyte antigen 4 (CTLA4) is one of the first negative regulators to be induced, and it directly competes with CD28 for the ligands CD80 and CD86. Programmed cell death protein 1 (PD1) is also expressed during T cell activation and counters positive signals through the TCR and CD28 by engaging its ligands programmed cell death 1 ligand 1 (PDL1) and/or PDL2 (referred to collectively here as PD1 ligands) [23–26]. These ‘coinhibitory’ receptors function as breaks for the adaptive immune response, serving as immune

checkpoints that effector T cells must pass in order to exert their full functions.

3. Methodology

3.1 Availability of PD-1 Binding Sites

In the first experiment, Geometric method was used to determine available binding sites of PD-1. The website <https://proteins.plus/> was used to determine all the binding sites of PD-1. The PDB code of PD-1, which is “3RRQ,” was entered into the “PDB-code” section. Then, “Go!” was pressed, leading to the “ProteinsPlus – Structure-Based Modeling Support Server,” which displayed an PD-1 model on the left and a list of options on the right. In the list of options to the right, “DoGSiteScorer Binding site detection” was selected. “DoGSiteScorer” was then selected and a list of options for settings appeared. The settings were set to as follows: for the “Analysis detail” section, “Pocket(s)” was chosen; for the “Binding site prediction granularity” section, “and druggability” was chosen; for the “Ligands” section, it was left blank; for the “Chain” section, “A” was chosen. After that, “calculate” was selected.

3.2 Virtual Screening of Potential Inhibitors of PD-1

In the second experiment, virtual screening was used to narrow to a smaller number of compounds that can potentially bind and inhibit PD-1. Virtual screening was based on pharmacophore maps, which are a presentation of a map of the interactions between two compounds. First, <http://pocketquery.csb.pitt.edu/> was used to determine the strength of the interaction between the compound tested and PD-1. After landing on the Pocket Query web page, “Search” was clicked and then “3BIK” was put into the “ID” section. The computer key “Enter” was clicked, yielding a list of clusters. For each cluster, the “export” button was clicked and then the “send to ZincPharmer” button was clicked. After landing in ZincPharmer for each cluster, the “Viewer” tab was clicked and then the “Receptor Residues” was made invisible. After that, the “Pharmacophore” tab was selected. Within the “Pharmacophore” tab, different

cluster groups were enabled and/or disabled, then the “submit query” button was selected to yield the number of hits found.

3.3 Evaluation of Selected Compounds Binding to PD-1

In the third experiment, the molecular docking approach can identify the degree of binding of each of the compounds from PocketQuery to PD-1. <http://www.swissdock.ch/docking#> was used to perform this procedure. On the SwissDock website, there are three sections to be filled: Target Selection, Ligand Selection and Description. For the “Target Selection” section, “upload file (max 5MB)” was selected. Then, the PDB file, the PDB code for PD-1 was uploaded to SwissDock. For the “Ligand Selection” section, the ZINC code for each compound was inputted into the text box. Then, yielding a new page containing all the ZINC AC hits found. The ligand that corresponded to the ZINC code was selected, and then the “Dock 1 selected ligand” button was clicked. Finally, in the “Description” section, the ZINC code for each compound was entered under the “Job Name (required)” section. Then, an E-mail address was inputted under the “E-mail address (optional)” section. “Start Docking” was selected. After a few hours, messages containing the link to each output of SwissDock were sent to the inputted E-mail address.

3.4 Identification of the Best Compound as Inhibitor of PD-1

In the fourth experiment, SwissADME was used to evaluate how five of the selected compounds based on the most negative ΔG fared with Lipinski’s rule. To start, <http://www.swissadme.ch/> was inputted into the search engine. Then, the SMILES code for each of the selected compounds is entered into the “Enter a list of SMILES here” section. Finally, “Run!” was clicked. Then, a detailed report about each compound was generated. The molecular weight, number of H-bond acceptors, number of H-bond donors, and $\text{Log } P_{o/w}$ (LogP) were recorded to determine if any aspect of Lipinski’s Rule of Five is violated.

4. Results and Discussion

4.1 Availability of PD-1 Binding Sites

In the first experiment, three methods were used to determine the available binding sites for PD-1. It would ensure that PD-1 has binding sites for identified inhibitors to bind. The Geometric method determines the binding sites based on the size and shape of PD-1. The website <https://proteins.plus/> was used because it incorporates the Geometric method when determining the binding sites to PD-1. Fig. 1 shows the binding sites of PD-1 determined using the Geometric method, and Table 1 shows the surface area and volume of binding sites.

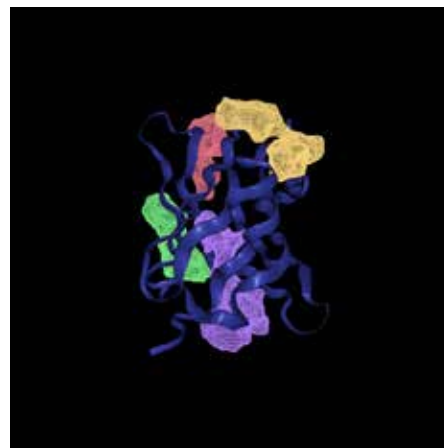




Figure 1. The binding sites of PD-1 determined using the Geometric method

Table 1. – The Surface Area and Volume of Binding Sites Determined by the Geometric Method

Name of binding site	Displayed color	Surface area(\AA^2)	Volume (\AA^3)
P_0		593.75	238.78
P_1		319.8	209.79
P_2		326.88	153.92
P_3		329.38	127.74

From these results, there are 4 available binding sites. It is notable that the binding site with the greatest surface area and volume is P_0, which has a surface area of 593.75\AA^2 and a volume of 238.78\AA^3 . The binding site with the smallest surface area is P_1, with 319.8\AA^2 . The binding site with the smallest volume is P_3, with 127.74\AA^3 . From the experimental results, we can conclude that PD-1 has numerous binding sites. It means that there are likely many opportunities to inhibit this protein, be it competitively or noncompetitively. However, there are only a very limited amount of inhibitors approved by the FDA.

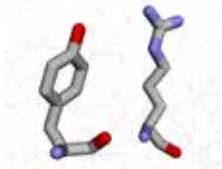
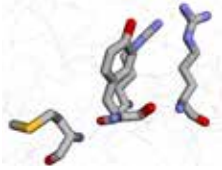
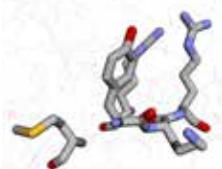
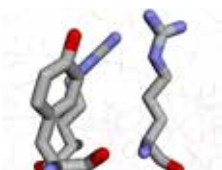
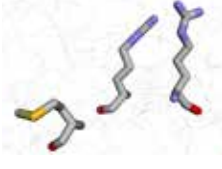
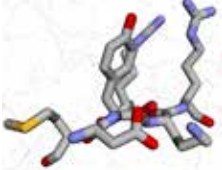
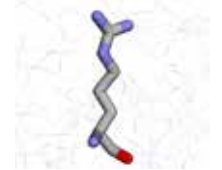
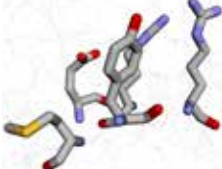
4.2 Virtual Screening of Potential Inhibitors of PD-1

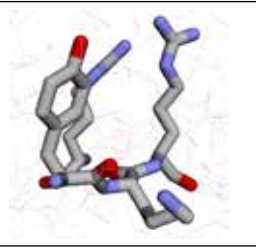
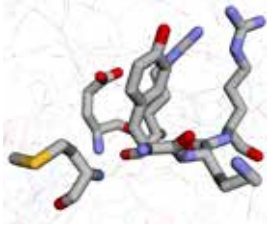
In the second experiment, <http://pocketquery.csb.pitt.edu/> was first used to show the strength of the interaction between the antibody and PD-1, and that strength is represented by a score. PocketQuery deter-

mines the strength of interaction by virtual screening and matching the compounds that may bind to PD-1 through pharmacophore maps. A pharmacophore map is a 3D representation of features that are critical for a ligand to interact with the target receptor of a specific binding site. The strongest interaction has a score of 1, with decreasing strengths leading to lower scores. Virtual screening was completed and ten clusters of chain A with the highest scores were selected. The scores, along with the models, amino acids, and sizes are showcased in (Table 2).

Table 2 shows that the first Chain A, consisting of TYR123 and ARG 125, has the highest score of 0.81099. This indicates the antibody and PD-1 have the strongest interaction. In comparison, the last Chain A consisting of GLU58, ARG 113, MET 115, TYR123 and ARG 125 has the lowest score of 0.680281. This indicates the antibody and PD-1 have the weakest interaction.

Table 2. – The Results of Virtual Screening of Potential Inhibitors of PD-1

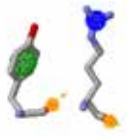

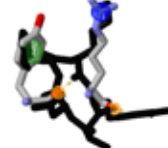
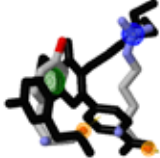
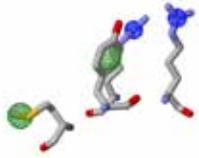
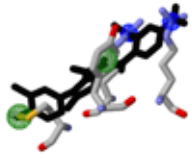
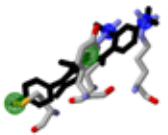
Chain 1	Size 2	Amino Acid 3	Score 4	Model 5
A	2	TYR123 ARG 125	0.81099	
A	4	ARG 113 MET 115 TYR123 ARG 125	0.740154	
A	5	ARG 113 MET 115 TYR123 LYS124 ARG 125	0.722176	
A	3	ARG 113 TYR123 ARG 125	0.705746	
A	3	ARG 113 MET 115 ARG 125	0.705299	
A	6	ARG 113 MET 115 ASP 122 TYR123 LYS124 ARG 125	0.701324	
A	1	ARG 125	0.693793	
A	5	GLU58 ARG 113 MET 115 TYR123 ARG 125	0.680281	

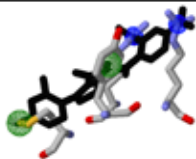
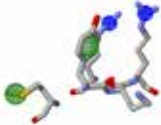
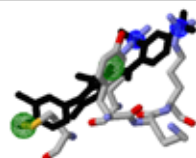
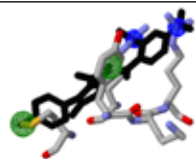
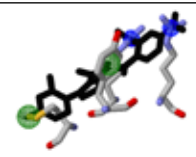
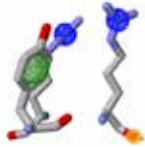
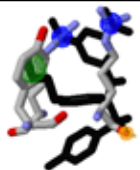

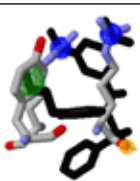
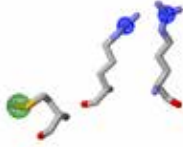
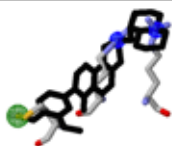
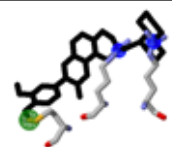
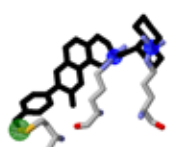
1	2	3	4	5
A	4	ARG 113 TYR123 LYS124 ARG 125	0.677142	
A	6	GLU58 ARG 113 MET 115 TYR123 LYS124 ARG 125	0.667507	

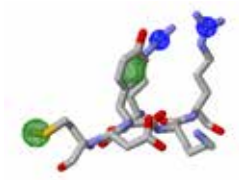
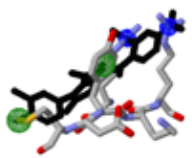
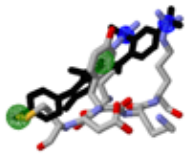
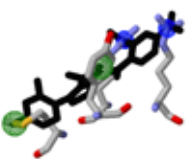




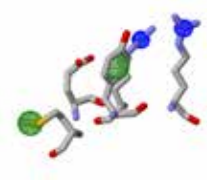
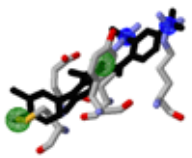
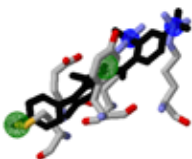
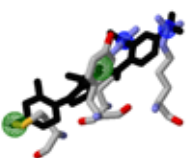
Each cluster will now be focused on individually to determine the hits that have the lowest RMSD scores, which indicate the hit that has the greatest overlap with the binding site of PD-1. The results are

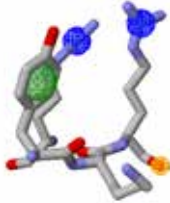
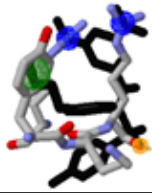
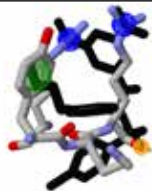
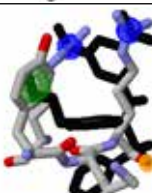
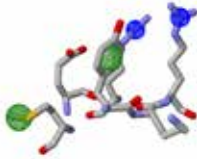
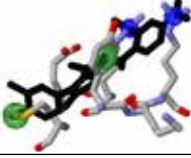

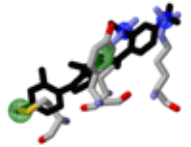
displayed in the table below. The structure in black represents the paired compound while the structure in gray represents the cluster. Table 3 shows each compound's RMSD score, name of hit, and model.

Table 3. – The RMSD Scores and the Model of 30 Selected Hits

Cluster Score + Model	Name of Hit	RMSD Score	Model
1	2	3	4
0.81099 	ZINC16267039	0.409	
	ZINC71788370	0.425	
	ZINC35326858	0.447	
0.740154 	ZINC02101516	0.183	
	ZINC02101503	0.184	

1	2	3	4
	ZINC02101649	0.188	
0.722176 	ZINC02101516	0.183	
	ZINC02101503	0.184	
	ZINC02101649	0.188	
0.705746 	ZINC40967643	0.189	
	ZINC40967646	0.190	
	ZINC40967640	0.190	
0.705299 	ZINC20762311	0.029	
	ZINC20761644	0.029	
	ZINC20762875	0.033	

1	2	3	4
0.701324 	ZINC02101516	0.183	
	ZINC02101503	0.184	
	ZINC02101649	0.188	
0.693793 	ZINC17020760	0.332	
	ZINC04899739	0.335	
	ZINC13541443	0.358	
0.680281 	ZINC02101516	0.183	
	ZINC02101503	0.184	
	ZINC02101649	0.188	

1	2	3	4
0.677142 	ZINC40967643	0.189	
	ZINC40967646	0.190	
	ZINC40967640	0.190	
0.667507 	ZINC02101516	0.183	
	ZINC02101503	0.184	
	ZINC02101649	0.188	

According to Table 3, the hits ZINC20762311 and ZINC20761644 from the cluster with a score of 0.705299 both have the lowest RMSD scores of 0.029. This represents an almost perfect overlap between the binding site and the hits. In contrast, the hit ZINC35326858 from the cluster with a score of 0.81099 has the highest RMSD score of 0.447. This means that the overlap is the least identical between the hit and PD-1.

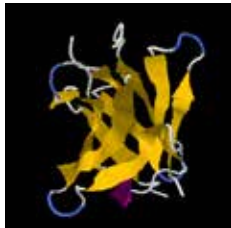
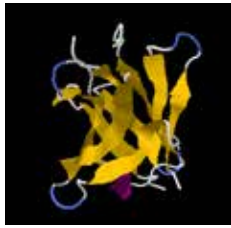
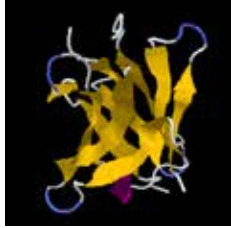



4.3 Evaluation of Selected Compounds Binding to PD-1

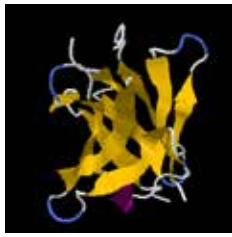
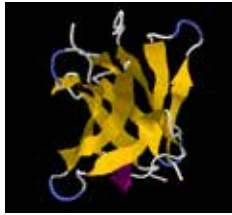
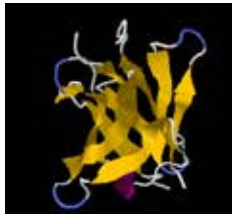

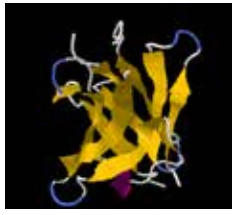
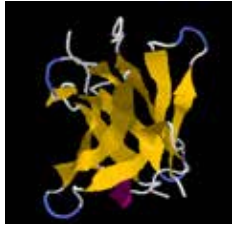

In the third experiment, the SwissDock server (<http://www.swissdock.ch/docking#>) was incorporated to determine which of the 15 identified

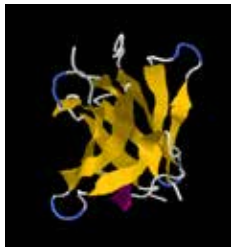
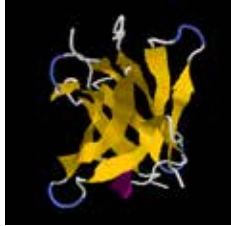
compounds is best able to bind to PD-1. SwissDock takes each of the 15 compounds and PD-1 and allows them to freely interact with each other. From this, SwissDock identifies the degree of interaction in all available binding sites. The output that SwissDock provides is the number of clusters, which indicates the number of binding sites; the number of elements, which indicates the number of positions the compound can interact with a specific binding site; the Full Fitness and Gibbs Free Energy (ΔG), which both quantify the favorability of the interaction. ΔG will be focused on instead of Full Fitness as it is more universally used by the scientific community. A more negative ΔG indicates a more favorable

interaction between the compound and PD-1. The results gathered are displayed in Table 4. It shows the models and estimated ΔG values for the 15 selected compounds.

Table 4. – Models and Estimated ΔG values for the 18 Selected Compounds

ZINC ID	Number of Clusters	Estimated ΔG (kcal/mol)	Model
<i>1</i>	<i>2</i>	<i>3</i>	<i>4</i>
ZINC16267039	31	-5.93	
ZINC71788370	29	-5.45	
ZINC35326858	30	-5.55	
ZINC02101516	32	-6.36	
ZINC02101503	33	-6.21	
ZINC02101649	33	-5.44	

1	2	3	4
ZINC40967643	33	-6.43	
ZINC40967646	31	-5.88	
ZINC40967640	30	-6.14	
ZINC20762311	31	-6.58	
ZINC20761644	32	-6.94	
ZINC20762875	31	-6.67	
ZINC17020760	36	-6.18	

1	2	3	4
ZINC04899739	30	-6.39	
ZINC13541443	31	-6.02	

From the results, the compound named ZINC20761644 has the most negative estimated ΔG of -6.94 kcal/mol. This suggests that ZINC20761644 binds to PD-1 the most favorably. The compound named ZINC02101649 has the lowest estimated ΔG of -5.44 kcal/mol. This suggests that ZINC02101649 binds to PD-1 the least favorably. From this, we can conclude that we do have compounds that are capable of binding to PD-1 and the most promising prospect is ZINC20761644. Furthermore, the range of clusters between the 15 compounds is 29 to 36.

4.4 Identification of the Best Compound as Inhibitor of PD-1

From the previous experiment, each compound's adherence to Lipinski's Rule of Five will be evaluated to determine the best compound to bind to PD-1. Lipinski's Rule of Five is used to evaluate a drug's viability in terms of absorption and permeation. The four requirements of Lipinski's Rule of Five are as follows: no more than five hydrogen bond donors, no more than ten hydrogen bond acceptors, calculated LogP of no greater than five and molecular mass of fewer than 500 daltons. Specifically, LogP determines the range of aqueous character and the lipid character, with a score having a positive relationship with the former and a negative relationship with the latter. Each compound is screened in the SwissADME server, which generates all the data needed to determine the conformity to Lipinski's Rule of Five. In Table 5, each component of Lipinski's Rule of Five is quantified by SwissADME and the conformity to Lipinski's Rule of Five is determined.

From the previous experiment, each compound's adherence to Lipinski's Rule of Five will be evaluated to determine the best compound to bind to PD-1. Lipinski's Rule of Five is used to evaluate a drug's viability in terms of absorption and permeation. The four requirements of Lipinski's Rule of Five are as follows: no more than five hydrogen bond donors, no more than ten hydrogen bond acceptors, calculated LogP of no greater than five and molecular mass of fewer than 500 daltons. Specifically, LogP determines the range of aqueous character and the lipid character, with a score having a positive relationship with the former and a negative relationship with the latter. Each compound is screened in the SwissADME server, which generates all the data needed to determine the conformity to Lipinski's Rule of Five. In Table 5, each component of Lipinski's Rule of Five is quantified by SwissADME and the conformity to Lipinski's Rule of Five is determined.

Table 5. – Analysis of Five Selected Compounds by SwissADME

ZINC Code	Molecular weight (g/mol)	Number of H-bond Acceptors	Number of H-bond Donors	Log P _{o/w} (iLOGP)	Conformity to Lipinski's Rule of Five
ZINC20761644	492.61	5	2	4.89	Yes
ZINC20762875	462.58	4	2	4.68	Yes
ZINC20762311	492.61	4	1	2.80	Yes
ZINC40967643	497.52	7	0	2.83	Yes
ZINC04899739	272.32	3	4	0.36	Yes

According to table 5, all five compounds adhere to Lipinski's Rule of Five. In this case, logically, the compound with the most negative estimated ΔG would serve as the best inhibitor for PD-1 because it has most favorable interactions with PD-1. The compound that would be the best inhibitor for PD-1. Therefore, it is ZINC20761644, and it has a ΔG of -6.94 kcal/mol.

5. Conclusion

In this research paper, the purpose was to identify new inhibitors of PD-1 that would serve as starting points to making more efficient inhibitors. These inhibitors would serve as therapeutics to prevent or cure cancer. The approach used was a series of computational studies. First, three methods were used to determine if there are sufficient binding sites for compounds to bind and inhibit PD-1. Then, a list of inhibitors was gathered through virtual screening in the PocketQuery and ZINCPharmer servers. Finally, the compound that would serve best as the inhibitor to PD-1 on the basis of energy of interaction and adherence to Lipinski's Rule was identified using SwissDock and SwissADME servers. The outcome from this computational study is a compound

known as ZINC20761644. From all the compounds favorable interactions with PD-1. Furthermore, ZINC20761644 satisfies Lipinski's Rule of Five, screened, ZINC20761644 has the most negative ΔG of -6.94 kcal/mol, indicating that it has the most signifying that it has the chemical and physical properties for it to serve as a therapeutic for human use.

The next step of this project is to test ZINC20761644 in a laboratory environment. Due to the COVID-19 pandemic, physical testing was not possible. However, physical testing is nevertheless an important part of validating the results obtained in this previous series of experiments as well as to further assess ZINC20761644 as a viable therapeutic for human use.

6. Acknowledgements

I would like to thank Dr. Moustafa Gabr for his consistent support, encouragement and patience throughout this project. I am also grateful that my parents lend me this opportunity to commit to Alzheimer's disease research.

7. Conflict of Interest

The authors declare no conflict of interest

References:

1. Zou W., Wolchok J. D., Chen L. PD-L1 (B7-H1) and PD-1 pathway blockade for cancer therapy: mechanisms, response biomarkers, and combinations. *Sci Transl Med.* 2016; 8: 328rv4.
2. Sun C., Mezzadra R., Schumacher T. N. Regulation and function of the PD-L1 checkpoint. *Immunity.*– 48: 2018: 434–52.
3. O'Sullivan Coyne G., Madan R. A., Gulley J. L. Nivolumab: promising survival signal coupled with limited toxicity raises expectations. *J Clin Oncol.*– 32: 2014: 986–8.
4. Wilkinson E. Nivolumab success in untreated metastatic melanoma. *Lancet Oncol.* 2015; 16: e9.
5. Naidoo J., Page D. B., Li B. T., Connell L. C., Schindler K., Lacouture M. E., et al. Toxicities of the anti-PD-1 and anti-PD-L1 immune checkpoint antibodies. *Ann Oncol.*– 26: 2015: 2375–91.
6. Topalian S. L., Drake C. G., Pardoll D. M. Immune checkpoint blockade: a common denominator approach to cancer therapy. *Cancer Cell.*– 27; 2015: 450–61.
7. Perez H. L., Cardarelli P. M., Deshpande S., Gangwar S., Schroeder G. M., Vite G. D., et al. Antibody–drug conjugates: current status and future directions. *Drug Discov Today.*– 19: 2014: 869–81.
8. Qian Wu1., Li Jiang1., Si-cheng Li1., Qiao-jun He1., Bo Y. ang1 and Ji Cao1. Small molecule inhibitors targeting the PD-1/PD-L1 signaling pathway. *Acta Pharmacologica* (2020) 0: 1–9.
9. Rosenberg S. A. IL-2: the first effective immunotherapy for human cancer. *J Immunol.*– 192(12): 2014: 5451–8.

10. Rotte A., Bhandaru M. Interleukin-2. Immunotherapy of melanoma. Cham: Springer International Publishing; 2016. *Rotte Journal of Experimental & Clinical Cancer Research* 38: 2019: 255–12.
 11. Rotte A., Bhandaru M. Interferon-a2b. Immunotherapy of melanoma. Cham: Springer International Publishing; 2016.
 12. Rotte A., Bhandaru M., Zhou Y., Mc Elwee K.J. Immunotherapy of melanoma: present options and future promises. *Cancer Metastasis Rev.*– 34(1): 2015; 115–28.
 13. Sanmamed M. F., Pastor F., Rodriguez A., Perez-Gracia J. L., Rodriguez-Ruiz M. E., Jure-Kunkel M., et al. Agonists of Co-stimulation in Cancer Immunotherapy Directed Against CD137, OX40, GITR, CD27, CD28, and ICOS. *Semin Oncol.*– 42(4): 2015: 640–55.
 14. Sanmamed M. F., Chen L. A Paradigm Shift in Cancer Immunotherapy: From Enhancement to Normalization. *Cell.*– 175(2): 2018; 313–26.
 15. Darvin P., Toor S. M., Sasidharan Nair V., Elkord E. Immune checkpoint inhibitors: recent progress and potential biomarkers. *Exp Mol Med.*– 50(12): 2018; 165.
 16. Looi C. K., Chung F. F., Leong C. O., Wong S. F., Rosli R., Mai C. W. Therapeutic challenges and current immunomodulatory strategies in targeting the immunosuppressive pancreatic tumor microenvironment. *J Exp Clin Cancer Res.*– 38(1): 2019; 162.
 17. Bhandaru M., Rotte A. Blockade of programmed cell death protein-1 pathway for the treatment of melanoma. *Journal of Dermatologic Research and Therapy.*– 1(2): 2017; 1–11.
 18. Wang X., Guo G., Guan H., Yu Y., Lu J., Yu J. Challenges and potential of PD-1 / PD-L1 checkpoint blockade immunotherapy for glioblastoma. *J Exp Clin Cancer Res.*– 38(1): 2019; 87.
 19. Hargadon K. M., Johnson C. E., Williams C. J. Immune checkpoint blockade therapy for cancer: An overview of FDA-approved immune checkpoint inhibitors. *Int Immunopharmacol.*– 62: 2018; 29–39.
 20. Rotte A., D’Orazi G., Bhandaru M. Nobel committee honors tumor immunologists. *J Exp Clin Cancer Res.*– 37(1): 2018; 262.
 21. Anand Rotte. Combination of CTLA-4 and PD-1 blockers for treatment of cancer. *Journal of Experimental & Clinical Cancer Research* – 38: 2019: 255–12.
 22. Greenwald R. J., Freeman G. J. & Sharpe A. H. The B7 family revisited. *Annu. Rev. Immunol.*– 23; 2005; 515–548.
 23. Latchman Y. et al. PD-L2 is a second ligand for PD-1 and inhibits T cell activation. *Nat. Immunol.*– 2. 2001. 261–268.
 24. Tseng S. Y. et al. B7-DC, a new dendritic cell molecule with potent costimulatory properties for T cells. *J. Exp. Med.*– 193. 2001: 839–846.
 25. Keir M. E., Butte M. J., Freeman G. J. & Sharpe A. H. PD-1 and its ligands in tolerance and immunity. *Annu. Rev. Immunol.*– 26. 2008; 677–704.
- Schildberg F. A., Klein S. R., Freeman G. J. & Sharpe A. H. Coinhibitory pathways in the B7-CD28 ligand-receptor family. *Immunity* – 44; 2016; 955–972.